Spectral Characterisation of Banded Iron Formations (BIFs) in Southern Bundelkhand Craton, India: Implications for Martian Surface Exploration

Shiwangee[1], Adnan Ahmad[2], Archana M. Nair[2]

[1] Department of Earth and Environmental Sciences, IISER Berhampur, India – 760003
[2] Earth System Science and Engineering, Department of Civil Engineering, IIT Guwahati, India – 781039

Keywords: Banded Iron Formations, Bundelkhand Craton, Mars, PRISMA, VNIR/SWIR spectroradiometer

Abstract

Banded Iron Formations (BIFs) are sedimentary rocks characterised by alternating bands of iron-rich layers and silica-rich layers. These formations, predominantly dating back to the Archean to Proterozoic eons, are one of the most significant lithologies in Precambrian sedimentary succession. Several studies have shown that during this time, both the planets, Earth and Mars, had similar atmospheric conditions, making BIFs a highly valuable source for future research in planetary geology. Their mineralogical and spectral properties serve as important analogues for comparing terrestrial BIFs with the iron-bearing formations on the Martian surface. The present study focuses on examining the spectral signatures of the BIFs of the southern part of the Bundelkhand Craton in Lalitpur, Uttar Pradesh, India. Since rocks and minerals show distinct absorption features due to their unique chemical composition, this work aims to identify and characterize the absorption features of minerals using a laboratory-based spectroradiometer. The spectral characteristics identified at the laboratory level are integrated with the hyperspectral remote sensing data analysis. The key absorption features for BIF samples were observed at 0.53 µm, 0.65 µm, 0.86 µm, primarily associated with ferric iron, and 1.4 µm, 1.9 µm, associated with the OH/H_2O group. PRISMA dataset from the study region was used to analyse and explore the BIF using advanced image analysis and spectral analysis techniques. This spectral study can provide a better understanding of Martian mineralogy, serving as a reference for future exploration with potential evidence of iron-rich mineralized microfossils embedded within the hematite deposits or silicified microfossils embedded in chert formations.

1. Introduction

Banded Iron Formations (BIFs) are sedimentary rocks composed of alternating bands of iron-rich layers and silica-rich layers. They represent one of the significant lithologies in the Precambrian sedimentary succession (~3800–543Ma) (Mukhopadhyay, 2019) and are characterized by the presence of thin layering in the rock. Most of the BIFs were formed between the ages of 3.8 and 1.8 billion years ago, spanning from Archean to Proterozoic eons, and are considered a key indicator of the early Earth processes (Crowley et al., 2008). Beyond their geological significance and being a significant source of iron ore, these formations are also believed to be linked with key processes such as the development of the oceanic circulation, the shifts in the oceanic circulation patterns, redox transition, microbial activities, and intersections with the hydrothermal systems (Mukhopadhyay, 2019; James, 1983). Their layered structures offer an insight into the ancient environmental cycle, and their study has broader implications for planetary exploration, identifying the biosignatures or sedimentary analogs on other planetary bodies like Mars.

Mars, positioned fourth in the order of the Sun, is approximately half the size of the Earth, often called 'Red Planet' due to its distinctive reddish appearance, a result of the iron oxide on its surface (Pabila, 2019), is today a deserted area and well known for its cold and arid climate (Pollack et al., 1987) primarily composed of CO_2 (carbon dioxide) making up 95.32% of its composition along with minor amounts of N_2 (nitrogen) and Ar (argon) at around 2.7 and 1.6 percent, respectively (Encrenaz, 2001). Figure 1 shows the topographic map of Mars, having a high-resolution shaded relief at a resolution of 0.125°, and is shown as a Mercator projection to a latitude of 70° north and south. From Archean to Proterozoic, the terrestrial atmosphere was changing from an anoxic condition to a more oxygenated stage, primarily due to photosynthetic organisms, with the atmosphere being significantly denser than today (Schelble et al., 2004; Bridges et al., 2008). It has therefore been proposed that Mars and Earth were more similar, had similar atmospheric conditions, and any potential life on Mars would likely resemble early terrestrial microorganisms (Rothschild, 2008; Nisbet & Fowler, 2003), making BIFs a highly valuable source for future research in planetary geology. The complex mineral evolution on Earth and its link with the biosphere (Hazen et al. 2008, 2011) may serve as a valuable analogy for the signs of life on the Martian planet. The detection of layered hematite and silica-rich deposits on the Martian surface has raised the possibility of the presence of banded iron formations (BIFs) (Christensen et al., 2000, 2001; Crowley et al., 2008). Terrestrial BIFs with their spectral features provide a robust framework and serve as valuable analogs for interpreting Martian hematite deposits and reconstructing paleoenvironmental conditions (Singh et al., 2015). Layered, crystalline gray hematite (α-Fe_2O_3) has been identified on the surface of Mars in Aram Chaos, Sinus Meridiani, and on various dispersed locations across the Valles Marineris region (Christensen et al., 2000, 2001).

In this study, the samples were collected by Dr. Sikha Hiloidari from the southern part of the Bundelkhand Craton in Lalitpur, Uttar Pradesh (Hiloidari et al., 2022), and were used to generate laboratory spectra. Further, the spectral signatures were examined using PRISMA (Hyperspectral Precursor of the Application Mission) datasets and the Lab Spectroradiometer. Multispectral datasets, due to their limited spectral resolution, are often insufficient for the identification of the diagnostic absorption features of rocks and minerals. Therefore, to overcome the limitation, we have incorporated a hyperspectral sensor (PRISMA), which provides continuous and narrow bands, allowing for a precise detection of distinct absorption features,

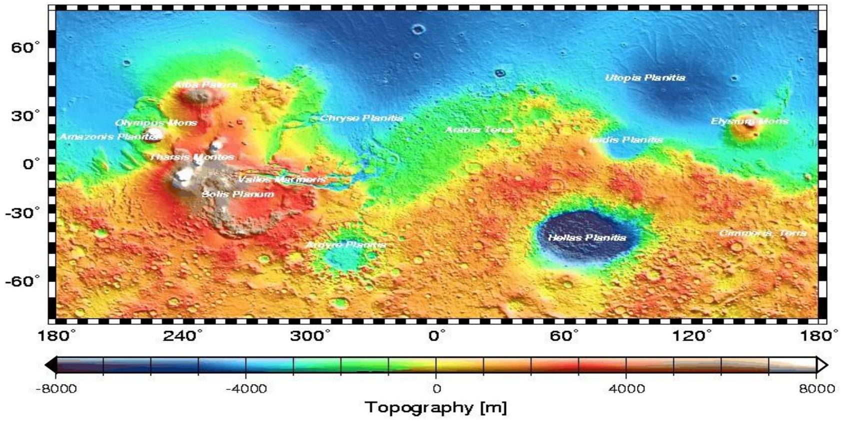

Figure 1. MOLA shaded relief topographic map of Mars with elevation in meters with Mercator projection. Credit: MOLA Science Team

thereby providing a better lithological and mineralogical understanding. A reflectance spectroradiometer is a well-known and widely accepted method used for mineral identification across various stages of mineral exploration. In the visible-near infrared (VNIR) and shortwave infrared (SWIR) regions (400–2500 nm) of reflectance spectroscopy, rocks and minerals show diagnostic absorption features allowing for their identification based on spectral signatures (Ahmad et al., 2022; Nair & Mathew, 2014). These absorption features arise from electronic transitions, vibrational modes, and charge transfer processes (Prado et al., 2016), which enable the identification and characterisation of rocks and minerals according to their spectral signature.

1.1 Study Area

This study focuses on the Girar Formation, situated in the southern region of Lalitpur, Uttar Pradesh, within the Bundelkhand geological zone (Fig. 2a). Spectral characterization of BIF samples has been implemented to interpret the sites as potential Martian analog sites. This study explores the possibility that, if ever life was present on the Martian Planet, it may have left behind evidence of iron-rich mineralized microfossils embedded within the hematite deposits or silicified microfossils embedded in chert formations. The Bundelkhand region (Fig. 2a) is in the Indian shield's north-central region, situated between 24°11'N-26 27'N and 78°10'E-81°24'E, having an exposed area of ~26,000 km^2 in the Indian subcontinent. Marginal basins dating back to the Paleoproterozoic era are distributed along the edges of the craton, including the Bijawar Basin in the southwest, the Sonrai Basin to the south, and the Gwalior Basin to the north (Hiloidari et al., 2022). The Vindhayan Supergroup overlies these peripheral basins except towards the north, where the region is blanketed by the Indo-Gangetic alluvial deposits (Hiloidari et al., 2022; Kaur et al., 2016). Five main lithological units make up the Bundelkhand massif: (1) the Paleo- to Neoarchean Bundelkhand Gneissic Complex, which includes tonalite–trondhjemite–granodiorite (TTG), gneisses, amphibolites, and granulites; 2) greenstone sequences of similar age, characterized by diverse mafic–ultramafic rocks, volcano-sedimentary assemblages, Banded Iron Formations (BIFs), and felsic volcanic units; (3) Neoarchean Bundelkhand granites that intrude both the TTG suites and greenstone belts; (4) The Madawara Ultramafic Complex; (5) Massive Proterozoic quartz reefs and mafic dykes were emplaced after the stabilization of the craton, associated with large-scale crustal extension and shear zones (Hiloidari et al., 2022). The samples have been collected from the Girar formation, which is exposed on the southern fringe of Bundelkhand Craton, situated in Lalitpur, Uttar Pradesh (Fig.2b). The Girar Formation mostly comprises Banded Iron Formations (BIFs), which are primarily Banded Magnetite Quartzite (BMQ) along with Banded Hematite Jaspillite (BHJ)and minor sulphide mineralisation (Hiloidari et al., 2022). Brecciated and mylonitized BIF were also present in some places, capped by a thin layer of quartzite or brecciated quartzite (Hiloidari et al., 2022).

2. Dataset and Methodology

2.1 PRISMA Dataset

Hyperspectral Precursor of the Application Mission (PRISMA) is a space initiative funded entirely by the Italian Space Agency, known as Agenzia Spaziale Italiana (ASI), which is a spaceborne sensor launched on March 22, 2019. It is an Earth Observation system that features a 30 km swath and 5-meter spatial resolution, combining a medium-resolution panchromatic camera with a hyperspectral sensor. The imaging spectrometer captures images with a 30-meter pixel size across a continuum of 230 spectral bands ranging from 0.4 µm to 2.5 µm, which acquires VNIR and SWIR regions (Guanter et al., 2015; Loizzo et al., 2018; Ahmad & Nair, 2024). The PRISMA L2D dataset has been utilised, which represents atmospherically and radiometrically corrected satellite imagery processed through a standardized pipeline tailored specifically for the PRISMA mission (Ahmad & Nair, 2024). Hyperspectral datasets are typically large datasets, which leads to increased complexity in data processing and handling. To manage and reduce this complexity, dimensionality reduction techniques are used to convert it into a lower-dimensional space while maintaining the crucial information. Before applying the Pixel Purity Index (PPI) to the PRISMA datasets, Principal Component Analysis (PCA) and Minimum Noise Fractionation (MNF) were conducted. PCA reduces dimensionality in the dataset and generates uncorrelated bands with maximized variance. This approach can create a smaller dataset while preserving a significant portion of the original spectral information, leading to uncorrelated PC bands (Richards et al., 1999). MNF is applied to hyperspectral data to reduce data dimensionality; therefore, minimizing the noise present in the dataset determines the inherent dimensionality of the image by filtering out noise and optimizing computational efficiency during further processing stages. Firstly, the noise is estimated in an image.

https://doi.org/10.5194/isprs-annals-X-5-W2-2025-597-2025

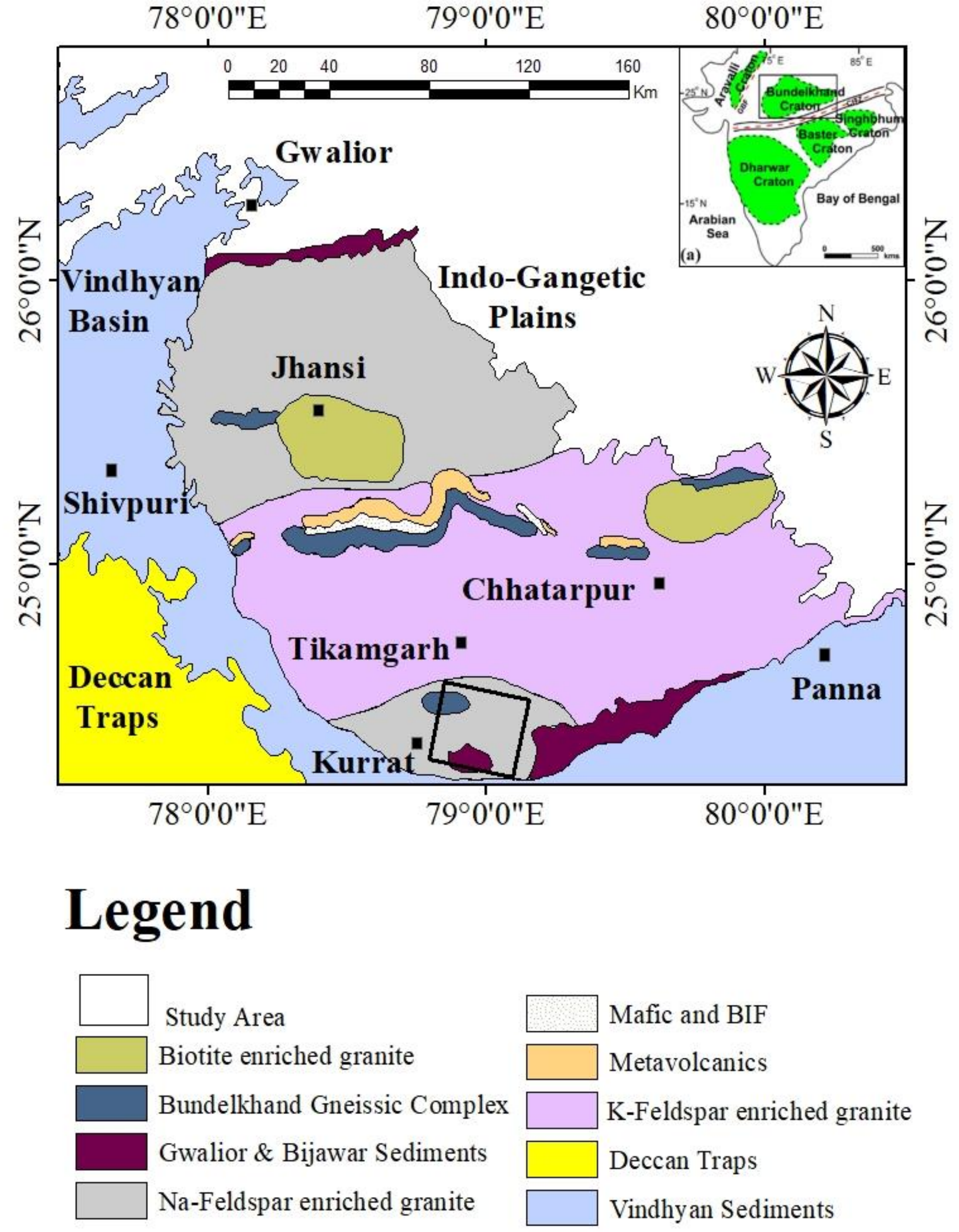

Figure 2. (a) Tectonic framework of the Indian Shield, highlighting the position of the Bundelkhand Craton. (b) The study area in Kurrat is depicted in a square box on the geological map of the Bundelkhand Craton (modified after Hiloidari et al., 2022)

The derived noise covariance matrix, which is a preliminary Principal Component (PC) transformation, is used to decorrelate and normalize the noise, ensuring that no correlation exists between the spectral bands in the dataset. After this, the second PC transformation takes place, which is applied to the output dataset from the first step, resulting in a set of bands that have been transformed using the MNF technique. It provides insights into the variance explained by each component, and based on the signal-to-noise ratio, higher eigenvalues correspond to a larger signal-to-noise ratio and vice versa. In the hyperspectral dataset, the Pixel Purity Index (PPI) is applied to the MNF bands to identify and extract the most spectrally pure pixels (Mishra et al., 2021). Pure pixels are those pixels that strongly represent individual materials or spectral signatures and are hence used for end-member extraction. A total of 10000 iterations were performed to compute the PPI (Ahmad & Nair, 2024; Boardman, 1993). The method selects the most distinct pixels and identifies them in *n*-dimensional space in a dataset. The scatter plot obtained helps to visualize how the shape of the data is distributed in spectral space (Kruse et al., 1997). Finally, Spectral Angle Mapper (SAM) operates on the principle of spectral similarity, comparing the spectral angle between two spectra to determine their similarity. It is a classification technique efficient in handling large-dimensional data. It measures the spectral angle by comparing the vector formed by the spectral signature, considering each as a point in a multi-dimensional space where the number of dimensions corresponds to the number of spectral bands. The smaller the angle between the pixel and the reference spectra, the greater the similarity and vice versa.

Mathematical Equation: - The spectral angle between two spectra can vary between 0 to π/2 (Mishra et al., 2021), and is calculated using the dot product formula:

$$\theta(x.y) = \cos^{-1}\left(\frac{\sum_{i=1}^{n} x_i y_i}{\left(\sum_{i=1}^{n} x_i^2\right)^{\frac{1}{2}} \times \left(\sum_{i=1}^{n} y_i^2\right)^{\frac{1}{2}}}\right) \quad (1)$$

Where: x represents the reference spectrum, y represents the spectrum of a pixel, and n represents the number of bands.

2.2 VNIR/SWIR Spectroradiometer

The samples of the BIF rocks were used to get the characteristic spectra in the VNIR/SWIR region by using an instrument manufactured by Spectra Vista Corporation named SVC-HR 768i spectroradiometer (Fig. 3). This device, made by Spectra Vista Corporation, uses three integrated spectrometers to measure the wavelengths ranging from 350 nm to 2500 nm. The rock spectra were acquired through two processes: (a) under laboratory conditions and (b) under controlled field conditions. For the laboratory condition, the spectra were taken in a dark room environment. The spectroradiometer was attached to the tripod in a manner that was approximately 1m above the samples for the spectral reading. A tungsten filament halogen lamp of 500-W was used as an artificial light source for the acquisition of the spectra. For the controlled field conditions, the instrument was kept under a stable, bright sunlight environment in such a manner that no shadow fell on the samples while taking the readings (Ahmad & Nair, 2024). Spectralon® panel, a 12 mm thick, low-density panel in a wooden box from Spectra Vista, was used as a reference before reading the targets.

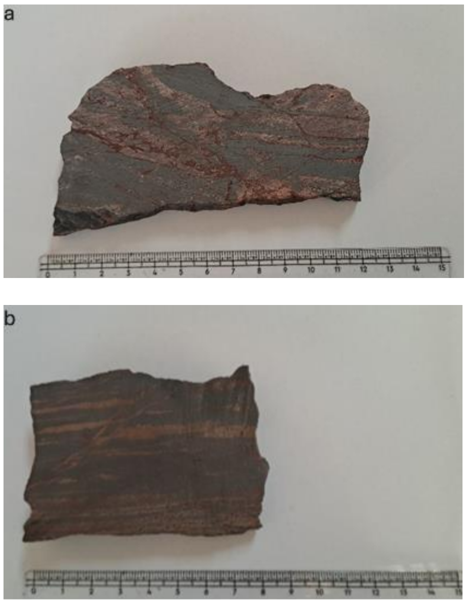

Figure 3. Field photographs of the BIF samples (a) BIF-2 and (b) BIF-1B collected from the southern region of Lalitpur, Uttar Pradesh, within the Bundelkhand Craton.

The rock samples' clear and fresh surfaces were considered for the reading. In total, two BIF samples (BIF-1B, BIF-2) were taken from the study region, and for each sample, ten different points were taken, with each point repeated three times for better precision in both field and lab conditions. After the spectral readings were taken, spectra for each of the three readings for a single point were averaged and then further resampled to PRISMA wavelength regions in ENVI software (Fig.5) to validate and compare them with the USGS standard spectra. It is often desirable to resample the spectral wavelength scale for better comparison with other datasets, as it interpolates the data points to a specified interval over a selected spectral range. Finally, the spectrum was plotted and matched using ENVI and Origin software.

Spectral Range	(350-2500) nm
Channels	768
Spectral Resolution	≤ 3.5nm, (700 nm) ≤16nm, (1500 nm) ≤14nm, (2100 nm)
Bandwidth	≤1.5nm, (350-1000 nm) ≤7.6 nm, (1000-1890 nm)
Field of View (FOV)	4° standard

Table 1. Specification of SVC-HR 768i Spectroradiometer

3. Results and Discussions

3.1 PRISMA Image Analysis

The BIF rock outcrops of the Girar formation of the Lalitpur region, situated in the southern part of the Bundelkhand region, were mapped using PRISMA in the VNIR region. With the help of PRISMA image-derived endmember extraction and applying the SAM, which classifies the image based on the angle between the reference spectra and from the PRISMA image, three distinctive endmembers were extracted, which include: vegetation, iron-bearing rocks (specifically hematite), and water bodies. The region exhibited moderate vegetation cover, resembling from the PRISMA image with the standard false color

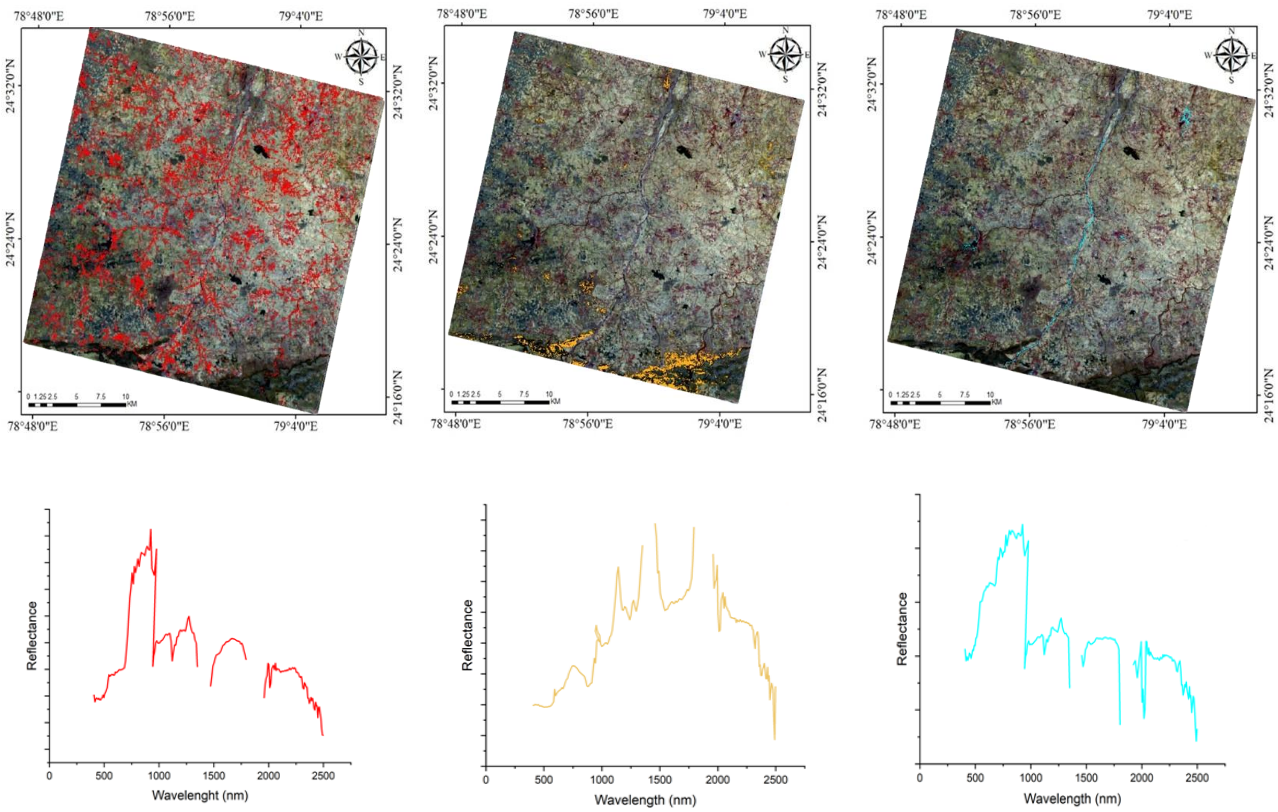

(a) (b) (c)

Figure 4. Image analysis using SAM technique overlaid on PRISMA FCC image (R: 785.65 nm, G: 684.13 nm, B: 519 nm) and respective PRISMA image derived spectra: (a) vegetation, (b) hematite, (c) water bodies.

composite (FCC) image (Fig. 4). This includes an absorption feature near 700 nm in the red region and a strong reflectance in the near-infrared (NIR) region, showing a close correspondence of the image-derived endmember with the Standard FCC image (Fig. 4a). In the VNIR SWIR region, BIFs with alternating bands of iron oxide and cherty quartz exhibit a distinctive absorption. The absorption feature at 535.08 nm and a minor feature at 861.45 nm, which is caused by a strong O^{2-}→Fe^{3+} charge transfer feature and crystal field transition (ligand field transition) of $Fe^{3+,}$ indicating the presence of hematite (Fig.4b) (Bell et al., 1990; Burns & R. G., 1993). The blue region indicates the presence of water (Fig. 4c) in the region with the spectral absorption feature at 1496.93 nm and 1958.62 nm, indicating the presence of H20 and OH/H_2O.

3.2 Laboratory-based Spectral Analysis

Laboratory-based spectroscopic analysis highlights the potential to characterise and differentiate their distinct spectral absorption features (Clark et al., 1990; Mishra et al., 2021). A spectral study aims to identify the diagnostic absorption features collected from the BIF samples. The spectral absorption feature obtained matches the absorption feature obtained from the spectral angle mapper technique applied to the PRISMA image. The spectra obtained from the samples show a strong match with Hematite (HS45.3) (Fig.6a), goethite (MPCMA2-B) (Fig.6b), and GDS76 (Fig.6c), of the USGS spectral library. Both samples show a common absorption feature at points 446.01nm, 475.32nm,

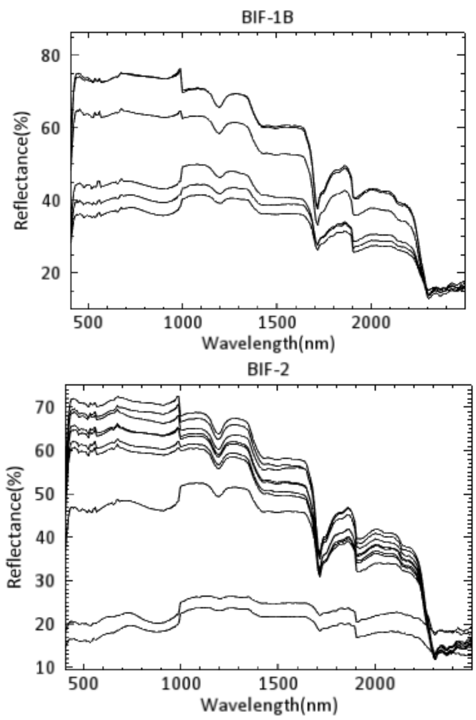

Figure 5. Spectral plot from BIF-1B and BIF-2 using the VNIR-SWIR spectroradiometer in the wavelength range 360 nm-2500nm.

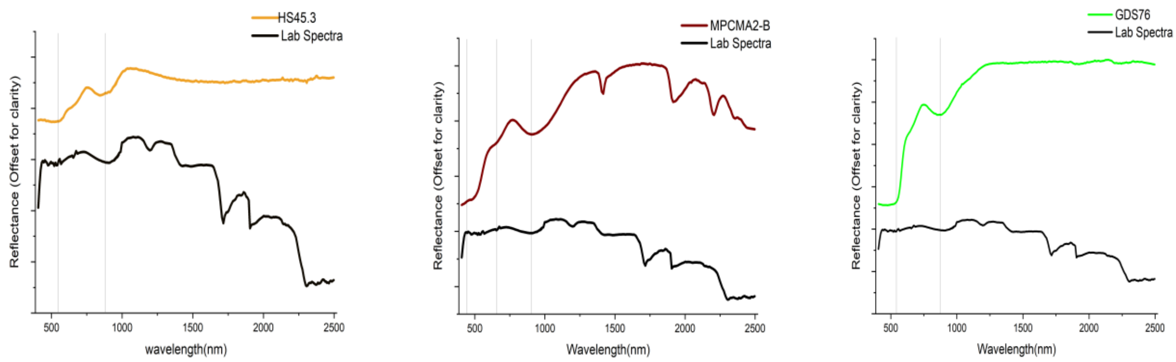

(a) (b) (c)

Figure 6. Spectral plot showing the match from the USGS spectra and lab spectroradiometer (a): Orange indicating hematite along with HS45.3 of the USGS spectra with absorption features matching at 535.05 nm, and 860.46 nm, (b): Deep red color indicating Goethite along with MPCMA2-B of the USGS spectra with absorption features matching at 446.01 nm, 655 nm, and 913.25 nm, (c) Green color matching GDS76 of the USGS spectral library which consist of 2% hematite (Fe_2O_3) and 98% quartz (SiO_2) with the lab spectra.

587.21 nm, 684.14 nm, 998.91 nm, 1196.84 nm, 1716.86 nm, 1904.93 nm, and 2305.72 nm. Hematite is the prevalent iron oxide present in the samples of BIF, with a weak absorption feature at 535.05nm due to the Fe-O charge transfer effect and a strong absorption feature at (881.46-913.45) nm due to ferric ion electronic transitions (Bell et al., 1990; Burns & R. G., 1993). The presence of Goethite can also be detected through the absorption feature observed at 446.01 nm, 655 nm, and 913.25 nm with MPCMA2-B of the USGS spectral library. The presence of a hydrous absorption band in the VIS-NIR spectral range confirms the presence of goethite in the BIF sample (Singh et al., 2015). Overall, several minor absorption features and a few major ones between 504.51 nm and 913.45 nm can be seen as matched with the standard USGS spectral library, denoting the presence of hematite and goethite. The GDS76 spectrum in the USGS spectral library includes 2% hematite (Fe_2O_3) and 98% quartz (SiO_2); the combined spectral data exhibit specific absorption features at 881.46 nm, which match the sample spectra exactly. Water absorption features can be observed at 1405.63 nm, 1416.54 nm, and 1904.93 nm due to the OH stretching overtone and the mixed band of H-O-H bending with OH stretching, respectively (Clark et al., 1990; Mishra et al., 2021). in BIF-2 and BIF-1B samples. The carbonate absorption feature can be seen around 2305.7 nm in both spectra of the samples.

4. Conclusion

This study employed an integrated approach combining hyperspectral remote sensing and laboratory-based spectroscopic methods to investigate the mineralogical characteristics of Banded Iron Formations (BIFs) and assess their potential analogues on Mars. The spectral analysis of the BIF samples collected from the Girar Formation, located in the southern region of Lalitpur, Uttar Pradesh, within the Bundelkhand geological zone, using remote sensing data and a spectroradiometer, enhances our understanding of the mineralized area by providing insights into the spatial distribution of the minerals present. This analysis confirmed the presence of iron-bearing minerals such as hematite, showing an absorption feature at 0.53 µm and 0.86 µm, and goethite at 0.46 µm and 0.65 µm, as well as water absorption features at 1.4 µm and 1.9 µm, by using a lab-based spectroradiometer and the remote sensing data acquired from the PRISMA sensor, which effectively identified diagnostic spectral features corresponding to these minerals. These minerals display diagnostic absorption features that help accurately characterize BIFs based on their spectral behaviour. The spectral characteristics identified in terrestrial BIFs can also be extended to the study of the Martian surface. The detection of hematite and associated minerals in Martian contexts emphasizes the importance of BIFs as analogues for planetary exploration, highlighting the potential for identifying iron-rich mineralized microfossils in hematite deposits or silicified microfossils in chert formations. Such findings reinforce hypotheses about past aqueous processes and possible habitability on Mars. Accordingly, this research provides a valuable reference for testing and calibration in ongoing Martian investigations, strengthening the connection between terrestrial analogue studies and extraterrestrial mineral exploration.

Acknowledgements

The authors express their sincere gratitude to IIT Guwahati for providing the necessary infrastructure to carry out the research. The first author expresses her gratitude to the Earth System Science and Engineering, Department of Civil Engineering, IIT Guwahati, and the Department of Earth and Environmental Sciences, IISER Berhampur for providing the opportunity to work to carry the dissertation work. The authors would also like to thank Dr. Sikha Hiloidari for providing rock samples for this study.

References

Ahmad, A., & Nair, A. M. (2024). Lithological mapping of charnockites using spectral mixture analysis. *Remote Sensing Applications: Society and Environment*, *34*, 101165.

Ahmad, A., & Nair, A. M. (2024). Spectral mixture analysis of intimate mixtures for lithological mapping. *ISPRS Journal of Photogrammetry and Remote Sensing*, *208*, 210-232.

Ahmad, A., Patel, R., Deka, B., Nagori, R., Arya, A. S., & Nair, A. M. (2022). Occurrence of secondary minerals at Tharsis Montes of Mars: A critical assessment. *Icarus*, *378*, 114953.

Bell III, J. F., McCord, T. B., & Owensby, P. D. (1990). Observational evidence of crystalline iron oxides on Mars. *Journal of Geophysical Research: Solid Earth*, *95*(B9), 14447-14461.

Boardman, J. W., Kruse, F. A., & Green, R. O. (1995, January). Mapping target signatures via partial unmixing of AVIRIS data. In *Summaries of the fifth annual JPL airborne earth science workshop. Volume 1: AVIRIS workshop*.

Burns, R. G. (1993). Origin of electronic spectra of minerals in the visible and near-infrared region. *Remote Geochemical Analysis*, 3-29.

Christensen, P. R., Bandfield, J. L., Clark, R. N., Edgett, K. S., Hamilton, V. E., Hoefen, T., ... & Smith, M. D. (2000). Detection of crystalline hematite mineralization on Mars by the Thermal Emission Spectrometer: Evidence for near-surface water. Journal of Geophysical Research: Planets, 105(E4), 9623–9642.

Christensen, P. R., Morris, R. V., Lane, M. D., Bandfield, J. L., & Malin, M. C. (2001). Global mapping of Martian hematite mineral deposits: Remnants of water-driven processes on early Mars. Journal of Geophysical Research: Planets, 106(E10), 23873-23885.

Clark, R. N., King, T. V., Klejwa, M., Swayze, G. A., & Vergo, N. (1990). High spectral resolution reflectance spectroscopy of minerals. *Journal of Geophysical Research: Solid Earth*, *95*(B8), 12653-12680.

Crowley, J. K., Hook, S. J., de Souza Filho, C. R., de Pereira Silva, G., Bridges, N. T., Thomson, B. J., ... & Marion, G. M. (2008, March). Spectral diversity of terrestrial banded iron formations and associated rocks: Implications for Mars remote sensing. In 39th Annual Lunar and Planetary Science Conference (No. 1391, p. 1263).

Encrenaz, T. (2001). The atmosphere of Mars as constrained by remote sensing. Space science reviews, 96(1), 411-424.

Guanter, L., Kaufmann, H., Segl, K., Foerster, S., Rogass, C., Chabrillat, S., ... & Sang, B. (2015). The EnMAP spaceborne imaging spectroscopy mission for earth observation. *Remote Sensing*, *7*(7), 8830-8857.

Hiloidari, S., Sarma, D. S., & Singh, S. P. (2022). Geochemical signatures and petrogenesis of Dhasan metabasalts from Kurrat–Girar–Badwar greenstone belt, southern Bundelkhand Craton, India. *Journal of Earth System Science*, *131*(4), 243.

Kaur, P., Zeh, A., Chaudhri, N., & Eliyas, N. (2016). Unravelling the record of Archaean crustal evolution of the Bundelkhand Craton, northern India using U–Pb zircon–monazite ages, Lu–Hf isotope systematics, and whole-rock geochemistry of granitoids. *Precambrian Research*, *281*, 384-413.

Kruse, F. A., Richardson, L. L., & Ambrosia, V. G. (1997, March). Techniques developed for geologic analysis of hyperspectral data applied to near-shore hyperspectral ocean data. In *Fourth International Conference on Remote Sensing for Marine and Coastal Environments, Orlando, Florida* (Vol. 17, p. 19).

Loizzo, R., Guarini, R., Longo, F., Scopa, T., Formaro, R., Facchinetti, C., & Varacalli, G. (2018, July). PRISMA: The Italian hyperspectral mission. In *IGARSS 2018-2018 IEEE international geoscience and remote sensing symposium* (pp. 175-178). IEEE.

Mishra, G., Govil, H., & Srivastava, P. K. (2021). Identification of malachite and alteration minerals using airborne AVIRIS-NG hyperspectral data. *Quaternary Science Advances*, *4*, 100036.
Mukhopadhyay, J. (2020). Archean banded iron formations of India. Earth-Science Reviews, 201, 102927.

Nair, A. M., & Mathew, G. (2014). Effect of bulk chemistry in the spectral variability of igneous rocks in VIS-NIR region: Implications to remote compositional mapping. International Journal of Applied Earth Observation and Geoinformation, 30, 227-237.

Nisbet, E. G., & Fowler, C. M. R. (2004). The early history of life. Biogeochemistry, 8, 1-39.

Pollack, J. B., Kasting, J. F., Richardson, S. M., & Poliakoff, K. (1987). The case for a wet, warm climate on early Mars. Icarus, 71(2), 203-224.

Prado, E. M. G., Silva, A. M., Ducart, D. F., Toledo, C. L. B., & de Assis, L. M. (2016). Reflectance spectroradiometry applied to a semi-quantitative analysis of the mineralogy of the N4ws deposit, Carajás Mineral Province, Pará, Brazil. Ore Geology Reviews, 78, 101-119.

Richards, J. A., & Jia, X. (1999). Error correction and registration of image data. In *Remote Sensing Digital Image Analysis: An Introduction* (pp. 39-74). Berlin, Heidelberg: Springer Berlin Heidelberg.

Rothschild, L. J. (2008). The evolution of photosynthesis… again?. Philosophical Transactions of the Royal Society B: Biological Sciences, 363(1504), 2787-2801.

Schelble, R. T., Westall, F., & Allen, C. C. (2004). ~ 1.8 Ga iron-mineralized microbiota from the Gunflint Iron Formation, Ontario, Canada: implications for Mars. Advances in Space Research, 33(8), 1268-1273.

Singh, M., Singhal, J., Prasad, K. A., Rajesh, V. J., Ray, D., & Sahoo, P. (2016). Spectral characteristics of banded iron formations in Singhbhum craton, eastern India: Implications for hematite deposits on Mars. Geoscience Frontiers, 7(6), 927-936